

## Electrochemically Stimulated pH Changes: A Route To Control Chemical Reactivity

Marco Frasconi, Ran Tel-Vered, Johann Elbaz, and Itamar Willner\*

*Institute of Chemistry, The Center for Nanoscience and Nanotechnology, The Hebrew University of Jerusalem, Jerusalem 91904, Israel*

Received November 8, 2009; E-mail: willnea@vms.huji.ac.il

**Abstract:** A bis-aniline-cross-linked Au nanoparticle (NP) composite is electrochemically prepared on a rough Pt film supported on a Au electrode. The electrochemical oxidation of the bis-aniline units to the quinoid state releases protons to the electrolyte solution, while the reduction of the quinoid bridges results in the uptake of protons from the electrolyte. By the cyclic oxidation of the bridging units ( $E = 0.25$  V vs SCE), and their reduction ( $E = -0.05$  V vs SCE), the pH of the solution could be reversibly switched between the values 5.8 and 7.2, respectively. The extent of the pH change is controlled by the number of electropolymerization cycles applied to synthesize the Au NP composite, demonstrating a ca. 1.5 pH units change by a matrix synthesized using 100 electropolymerization cycles. The pH changes are used to reversibly activate and deactivate a C-quadruplex (i-motif)-bridged  $Mg^{2+}$ -dependent DNAzyme.

### Introduction

The pH of aqueous environments controls numerous chemical and biological transformations.<sup>1</sup> For example, pH changes control the fluorescence quenching of chromophores, and this feature was used to develop molecular switches<sup>2</sup> and logic gates.<sup>3</sup> Similarly, pH changes were used to drive molecular machinery functions<sup>4</sup> and controlled release processes.<sup>5</sup> Other pH-controlled processes include the switchable gel-to-solid phase transition of polymers,<sup>6</sup> the aggregation/deaggregation of

amphiphilic structures,<sup>7</sup> and the electrostatic assembly of molecules, nanoparticles and polyelectrolytes on charged surfaces.<sup>8</sup> Also, different biological transformations, such as biocatalyzed transformations,<sup>9</sup> dissociation of duplex DNA, or the self-assembly of i-motif (C-quadruplex) structures,<sup>10</sup> are controlled by pH.

The pH-controlled electrochemical activation of numerous redox-active substrates is a basic characteristic of many molecular or polymer systems.<sup>11</sup> Different applications of pH-regulated electrochemical processes, such as the development of molecular switches<sup>12</sup> or “smart” electrochemical sensors,<sup>13</sup> were suggested. While the effect of pH on the electroactivity of molecular substrates is well established, the reverse process,

- (1) (a) Boyer, P. D. *Annu. Rev. Biochem.* **1997**, *66*, 717–749. (b) Verkhovskiy, M. I.; Jasaitis, A.; Verkhovskaya, M. L.; Morgan, J. E.; Wilkström, M. *Nature* **1999**, *400*, 480–483. (c) Yoshida, M.; Muneyuki, E.; Hisabori, T. *Nat. Rev. Mol. Cell Biol.* **2001**, *2*, 669–677. (d) Blair, D. F. *FEBS Lett.* **2003**, *545*, 86–95.
- (2) (a) de Silva, S. A.; Loo, K. C.; Amorelli, B.; Pathirana, S. L.; Nyakirang'ani, M.; Dharmasena, M.; Demarais, S.; Dorcley, B.; Pullay, P.; Salih, Y. A. *J. Mater. Chem.* **2005**, *15*, 2791–2795. (b) Koo, C.-K.; Lam, B.; Leung, S.-K.; Lam, M. H.-W.; Wong, W.-Y. *J. Am. Chem. Soc.* **2006**, *128*, 16434–16435. (c) Silvi, S.; Arduini, A.; Pochini, A.; Secchi, A.; Tomasulo, M.; Raymo, F. M.; Barboncini, M.; Credi, A. *J. Am. Chem. Soc.* **2007**, *129*, 13378–13379.
- (3) (a) de Silva, A. P.; McClenaghan, N. D. *Chem.—Eur. J.* **2004**, *10*, 574–586. (b) Silvi, S.; Constable, E. C.; Housecroft, C. E.; Beves, J. E.; Dunphy, E. L.; Tomasulo, M.; Raymo, F. M.; Credi, A. *Chem.—Eur. J.* **2009**, *15*, 178–185.
- (4) (a) Barboiu, M.; Lehn, J.-M. *Proc. Natl. Acad. Sci. U.S.A.* **2002**, *99*, 5201–5206. (b) Badjic, J. D.; Balzani, V.; Credi, A.; Silvi, S.; Stoddart, J. F. *Science* **2004**, *303*, 1845–1849. (c) Kay, E. R.; Leigh, D. A.; Zerbetto, F. *Angew. Chem., Int. Ed.* **2007**, *46*, 72–191. (d) Wu, J.; Leung, K. C.-F.; Benítez, D.; Han, J.-Y.; Cantrill, S. J.; Fang, L.; Stoddart, J. F. *Angew. Chem., Int. Ed.* **2008**, *47*, 7470–7474.
- (5) (a) Murthy, N.; Xu, M.; Schuck, S.; Kunisawa, J.; Shastri, N.; Fréchet, J. M. J. *Proc. Natl. Acad. Sci. U.S.A.* **2003**, *100*, 4995–4500. (b) Fattal, E.; Couvreur, P.; Dubernet, C. *Adv. Drug Delivery Rev.* **2004**, *56*, 931–946. (c) Bachelier, E. M.; Beaudette, T. T.; Broaders, K. E.; Dashe, J.; Fréchet, J. M. J. *J. Am. Chem. Soc.* **2008**, *130*, 10494–10495. (d) Khashab, N. M.; Belowich, M. E.; Trabolsi, A.; Friedman, D. C.; Valente, C.; Lau, Y.; Khatib, H. A.; Zink, J. I.; Stoddart, J. F. *Chem. Commun.* **2009**, 5371–5373.
- (6) (a) Shen, X.; Zhang, L.; Jiang, X.; Hu, Y.; Guo, J. *Angew. Chem., Int. Ed.* **2007**, *46*, 7104–7107. (b) Suzuki, T.; Karino, T.; Ikkai, F.; Shibayama, M. *Macromolecules* **2008**, *41*, 9882–9889.
- (7) (a) Marquez, C.; Nau, W. M. *Angew. Chem., Int. Ed.* **2001**, *40*, 3155–3160. (b) Minkenberg, C. B.; Florusse, L.; Eelkema, R.; Koper, G. J. M.; van Esch, J. H. *J. Am. Chem. Soc.* **2009**, *131*, 11274–11275.
- (8) (a) Matthews, J. R.; Tuncel, D.; Jacobs, R. M. J.; Bain, C. D.; Anderson, H. L. *J. Am. Chem. Soc.* **2003**, *125*, 6428–6433. (b) La Spina, R.; Tomlinson, M. R.; Ruiz-Pérez, L.; Chiche, A.; Langridge, S.; Geoghegan, M. *Angew. Chem., Int. Ed.* **2007**, *46*, 6460–6463.
- (9) Marangoni, A. G. pH Dependence of Enzyme Catalyzed Reactions. *Enzyme Kinetics: A Modern Approach*; John Wiley and Sons, Inc.: Hoboken, NJ, 2003; Chapter 6.
- (10) (a) Liu, D. S.; Balasubramanian, S. *Angew. Chem., Int. Ed.* **2003**, *42*, 5734–5736. (b) Liedl, T.; Simmel, F. C. *Nano Lett.* **2005**, *5*, 1894–1898. (c) Liu, D. S.; Bruckbauer, A.; Abell, C.; Balasubramanian, S.; Kang, D.-J.; Klenerman, D.; Zhou, D. *J. Am. Chem. Soc.* **2006**, *128*, 2067–2071.
- (11) (a) Shu, C. F.; Wrighton, M. S. *J. Phys. Chem.* **1988**, *92*, 5221–5229. (b) Niwa, M.; Mori, T.; Higashi, N. *Macromolecules* **1995**, *28*, 7770–7774. (c) Doron, A.; Katz, E.; Tao, G.; Willner, I. *Langmuir* **1997**, *13*, 1783–1790. (d) Bartlett, P. N.; Grossel, M. C.; Barrios, E. M. *J. Electroanal. Chem.* **2000**, *487*, 142–148.
- (12) (a) Katz, E.; Lion-Dagan, M.; Willner, I. *J. Electroanal. Chem.* **1996**, *408*, 107–112. (b) Zhou, J.; Wang, G.; Hu, J.; Lu, X.; Li, J. *Chem. Commun.* **2006**, 4820–4822.
- (13) (a) Hickman, J. J.; Ofer, D.; Laibinis, P. E.; Whitesides, G. M.; Wrighton, M. S. *Science* **1991**, *252*, 688–691. (b) Doron, A.; Portnoy, M.; Lion-Dagan, M.; Katz, E.; Willner, I. *J. Am. Chem. Soc.* **1996**, *118*, 8937–8944. (c) Robinson, K. L.; Lawrence, N. S. *Anal. Chem.* **2006**, *78*, 2450–2455.

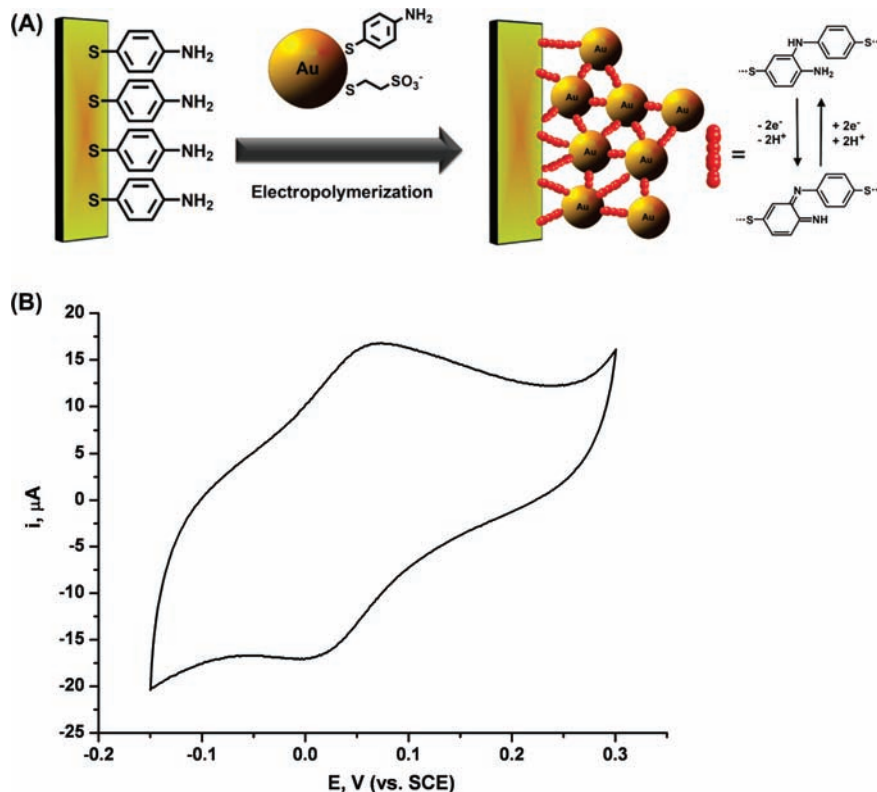


**Figure 1.** (A) Schematic presentation of the electropolymerization of the bis-aniline-cross-linked Au NP composite and the generation of electrochemically induced pH changes in aqueous solutions. (B) Cyclic voltammogram corresponding to the bis-aniline-cross-linked Au NP composite-modified Au electrode, generated by 100 electropolymerization cycles, in 0.5 M NaCl. Scan rate is 100 mV s<sup>-1</sup>.

namely, the electrochemical stimulation of pH changes in aqueous media by the redox activation of molecular assemblies, and the use of these pH changes to trigger chemical processes are relatively unexplored. Different methods to control the pH of aqueous solutions were suggested, including the constant potential electrolysis of water<sup>14</sup> or the use of electrodes modified with conductive polymers,<sup>15</sup> but these methods lead only to small pH changes and are either of poor reversibility or involve the degradation of the components of the electrochemical cell.

In a series of recent reports, we have demonstrated the electrochemical synthesis of metal nanoparticles (NPs) composites on Au electrode surfaces.<sup>16,17</sup> According to this approach, thioaniline-functionalized metal NPs, e.g., Au NPs<sup>16</sup> or Pt NPs<sup>17</sup> were electropolymerized on a thioaniline monolayer-modified Au electrode to yield a three-dimensional bis-aniline-cross-linked metal NP composite. These NP composites were used as sensing matrices. For example, the Au NP-modified electrode was used for the electrochemical<sup>16a</sup> or surface plasmon reso-

nance (SPR)<sup>16b</sup> detection of trinitrotoluene (TNT). Also, the 3D Pt NP composite was used for the electrochemical detection of H<sub>2</sub>O<sub>2</sub>.<sup>17</sup> This method to electropolymerize Au NPs on electrodes was further developed to coelectropolymerize Au NPs and enzymes on electrodes or Au NPs and semiconductor NPs on electrode supports, and the resulting hybrid systems were used as amperometric biosensors,<sup>16</sup> or photoelectrochemical electrodes.<sup>18</sup>

In the present study we use electropolymerization to synthesize a bis-aniline-cross-linked Au nanoparticle (NP) composite on an electrode and demonstrate the reversible electrostimulated pH change in a solution through oxidation/reduction of the bis-aniline bridging units. We show that, upon the appropriate nanoengineering of the electrode, we switch the pH of the solution by ca. 1.5 units. The pH changes are implemented for the cyclic electrochemical activation and deactivation of a Mg<sup>2+</sup>-dependent DNAzyme through the pH-induced formation and separation of i-motif complexes, respectively.

## Results and Discussion

The thioaniline-functionalized Au NPs were electropolymerized, as previously reported, to yield the three-dimensional bis-aniline-cross-linked Au NP composite on a Au-coated glass surface, Figure 1A. The thickness of the Au NP composite, upon the application of 60 electropolymerization cycles, corresponded to ca. 10 nm, a value that translates to three random densely packed layers of NPs.<sup>16b</sup> The bis-aniline bridging units of the Au NP composite exhibit quasi-reversible redox properties,  $E^{\circ} = 0.05$  V vs SCE at pH = 7.2, Figure 1B. The oxidation of the

- (14) (a) Hamann, C. H.; Roepke, T.; Schmittinger, P. In *Encyclopedia of Electrochemistry*; Bard, A. J., Stratmann, M., Eds; Wiley-VCH: Weinheim, Germany, 2007; Vol. 10, Chapter 5. (b) Morimoto, K.; Toya, M.; Fukuda, J.; Suzuki, H. *Anal. Chem.* **2008**, *80*, 905–914. (c) Kao, L. T.-H.; Hsu, H.-Y.; Grätzel, M. *Anal. Chem.* **2008**, *80*, 4065–4069.
- (15) (a) Okano, M.; Fujishima, A.; Honda, K. *J. Electroanal. Chem.* **1985**, *185*, 393–396. (b) Shinohara, H.; Kojima, J.; Aizawa, M. *J. Electroanal. Chem.* **1989**, *266*, 297–308.
- (16) (a) Riskin, M.; Tel-Vered, R.; Bourenko, T.; Granot, E.; Willner, I. *J. Am. Chem. Soc.* **2008**, *130*, 9726–9733. (b) Riskin, M.; Tel-Vered, R.; Lioubashevski, O.; Willner, I. *J. Am. Chem. Soc.* **2009**, *131*, 7368–7378. (c) Yehezkeili, O.; Yan, Y.-M.; Baravik, I.; Tel-Vered, R.; Willner, I. *Chem.—Eur. J.* **2009**, *15*, 2674–2679.
- (17) Bahshi, L.; Frascioni, M.; Tel-Vered, R.; Yehezkeili, O.; Willner, I. *Anal. Chem.* **2008**, *80*, 8253–8259.

- (18) Yildiz, H. B.; Tel-Vered, R.; Willner, I. *Adv. Funct. Mater.* **2008**, *18*, 3497–3505.

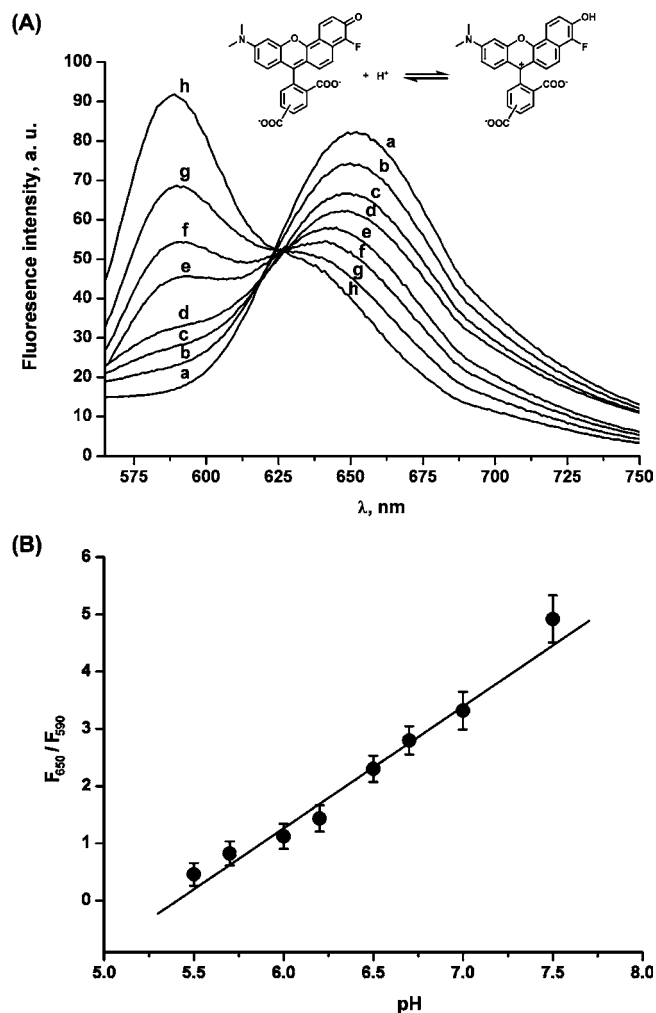


**Figure 2.** (A) Emission spectra corresponding to the carboxy seminaphthorhodafluors (carboxy SNARFs) dye, 5  $\mu$ M, in a phosphate buffer, 50 mM, that included NaCl, 450 mM, at variable pH values: (a) 7.5, (b) 7.0, (c) 6.7, (d) 6.5, (e) 6.2, (f) 6.0, (g) 5.7, (h) 5.5. Excitation wavelength  $\lambda_{\text{ex}} = 561$  nm. The pH of the solution was adjusted by using HCl. (B) Calibration curve correlating the fluorescence intensities ratio at  $\lambda_1 = 650$  nm/ $\lambda_2 = 590$  nm to the pH of the solution.

bridges to the quinoid state releases protons, while the reduction of the quinoid bridges involves the uptake of protons from the aqueous medium. Thus, by the reversible oxidation and reduction of the bridging units, the pH of the aqueous electrolyte solution can be switched between lower and higher values, respectively.

The pH of the aqueous electrolyte solution was probed by using carboxy seminaphthorhodafluors (carboxy SNARFs) as a fluorescent pH indicator.<sup>19</sup> Figure 2A shows the fluorescence spectra of carboxy SNARFs at different pH values. At pH = 7.5, the indicator exhibits a fluorescence band at  $\lambda_{\text{max}} = 650$  nm. Upon the chemical acidification of the system, the intensity of this band decreases with the concomitant buildup of a new fluorescence band at  $\lambda_{\text{max}} = 590$  nm, and at pH = 5.5, the intensity of this band predominates. The derived calibration curve is depicted in Figure 2B, implying that the intensities ratio of the two fluorescence maxima,  $F_{650}/F_{590}$ , provides a delicate indicator for the pH of the aqueous medium.

The content of the bis-aniline-bridged Au NP composite associated with the electrode is expected to be controlled by the number of electropolymerization cycles. Figure S1, Supporting Information, depicts the fluorescence spectra changes of the pH indicator carboxy SNARFs, upon synthesizing Au NP composites using variable numbers of electropolymerization cycles and applying an oxidation pulse from  $-0.05$  to  $0.25$  V vs SCE on the electrode. This potential pulse is expected to oxidize the bridging units and, thus, acidify the electrolyte solution. As can be seen, indeed, the fluorescence band at  $\lambda = 650$  nm decreases, while the band at  $\lambda = 590$  nm increases, as the number of electropolymerization cycles (the content of bridged Au NPs) is elevated. The formation of the band at  $\lambda = 590$  nm and the depletion of the band at  $\lambda = 650$  nm are consistent with the acidification of the electrolyte solution and the release of protons upon oxidation of the bridging units. Figure 3A shows the pH changes in the electrolyte solution upon oxidizing the bridging units of the Au NP composites, generated by variable numbers of electropolymerization cycles. We realize that the composites generated by 60 or more electropolymerization cycles yield a pH change of ca.  $\Delta\text{pH} = 0.5$ . Albeit the results demonstrate that the bridged Au NP composite allows the electrostimulated change of the pH, the pH change is too small to enable the secondary control of chemical processes. To enhance the electrogenerated pH changes, we searched for means to elevate the content of the bis-aniline-cross-linked Au NPs associated with the electrode. Toward this goal, we roughened the Au electrode surface by the electrochemically induced deposition of Pt black on the electrode surface. This was carried out by applying a constant voltage on the Au electrode,  $E = -0.75$  V vs a Pt wire, in a solution containing 5 mM  $\text{K}_2\text{PtCl}_6$  in 0.2 M  $\text{H}_2\text{SO}_4$ , for 60 s. The surface area of the deposited Pt black matrix was ca. 11-fold higher than that of the bare Au electrode. After the functionalization of the Pt black with the thioaniline monolayer, the bis-aniline-bridged Au NP composite was synthesized by the electrochemical deposition of the thioaniline-functionalized Au NPs on the thioaniline-monolayer-modified Pt black support. Figure 3B depicts the fluorescence spectra of the pH indicator upon applying an oxidation pulse on Pt black-coated electrodes modified with the bridged Au NP composites, which were synthesized by variable numbers of electropolymerization cycles. As the number of electropolymerization cycles is elevated, the fluorescence band at  $\lambda = 650$  nm decreases, while the fluorescence intensity at  $\lambda = 590$  nm is intensified. Using the calibration curve reported in Figure 2B and the fluorescence intensity changes at these two bands, we derived the curve that corresponded to the electrostimulated pH changes in the electrolyte solution with respect to the different number of electropolymerization cycles, Figure 3C. Evidently, the composite generated by the application of 100 electropolymerization cycles leads to a pH change of  $\Delta\text{pH} = 1.4$  (for the translation of the  $\Delta\text{pH}$  into moles of  $\text{H}_3\text{O}^+$ , see Supporting Information, Figure S2).

The electrostimulated pH changes in the electrolyte solution are reversible, Figure 4. By the cyclic application of oxidative ( $E = 0.25$  V vs SCE) or reductive ( $E = -0.05$  V vs SCE) potential pulses on the bis-aniline-cross-linked Au NP electrode, with the corresponding current responses shown in Figure 4A, the pH of the electrolyte is switched between the values of 5.8 and 7.2, respectively. Figure 4B shows the fluorescence spectra of the dye indicator upon applying several consecutive oxidation–reduction potential steps on the functionalized

(19) Marcotte, N.; Brouwer, A. M. *J. Phys. Chem. B* **2005**, *109*, 11819–11828.

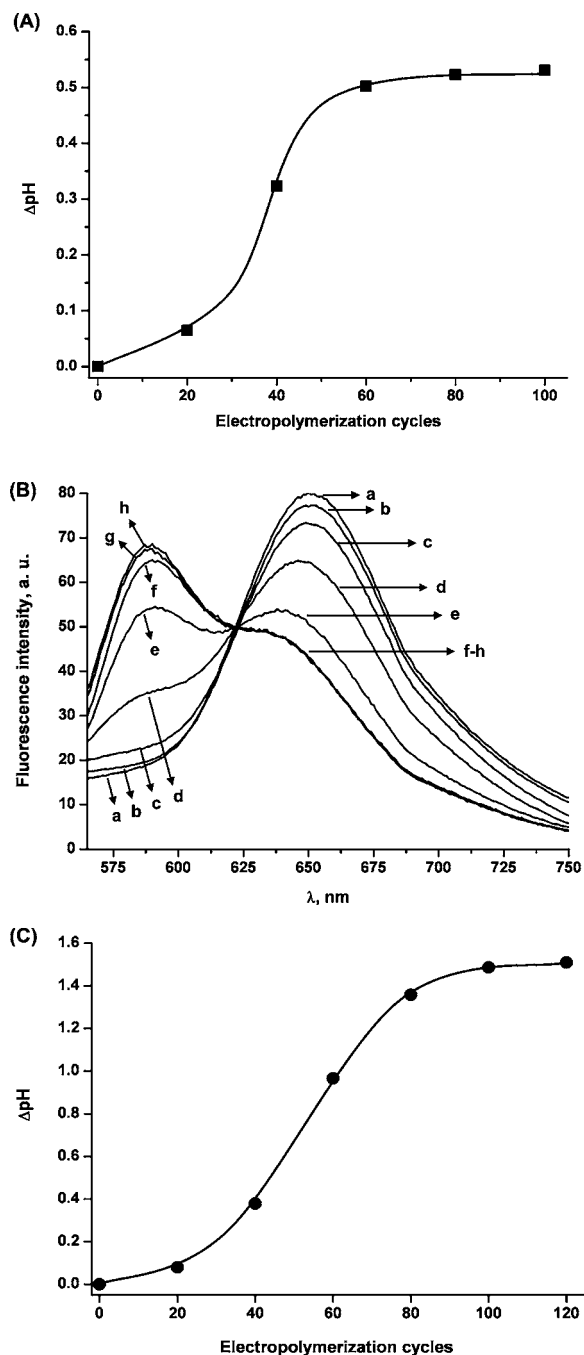


**Figure 3.** (A) Electrostimulated pH changes generated by the bis-aniline-cross-linked Au NPs electropolymerized composite associated with the Au electrode generated by the application of variable numbers of electropolymerization cycles. The pH values were derived from the emission intensities ratio at  $\lambda_1 = 650 \text{ nm}/\lambda_2 = 590 \text{ nm}$ , associated with the carboxy SNARFs dye. (B) Fluorescence spectra corresponding to electrostimulated pH changes by the bis-aniline-cross-linked Au NPs electropolymerized composite generated by variable numbers of electropolymerization cycles on a Pt black-coated Au electrode: (a) 0 (b) 20, (c) 40, (d) 60, (e) 80, (f) 100, (g) 120, (h) 140 cycles. (C) Electrostimulated pH changes generated by the bis-aniline-cross-linked Au NPs electropolymerized composite prepared by variable numbers of electropolymerization cycles on a Pt black-coated Au electrode. The pH values were derived from the emission intensities ratio at  $\lambda_1 = 650 \text{ nm}/\lambda_2 = 590 \text{ nm}$  associated with the carboxy SNARFs dye. In all measurements the spectra were recorded following the application of an oxidation potential pulse on the electrode,  $E = 0.25 \text{ V vs SCE}$ , for 30 s. Excitation wavelength  $\lambda_{\text{ex}} = 561 \text{ nm}$ . A  $100 \mu\text{L}$  solution containing carboxy SNARFs dye,  $5 \mu\text{M}$ , in a  $0.5 \text{ M NaCl}$  solution was used. In all of the experiments the volume of the solution in which the pH was altered corresponded to  $100 \mu\text{L}$ .

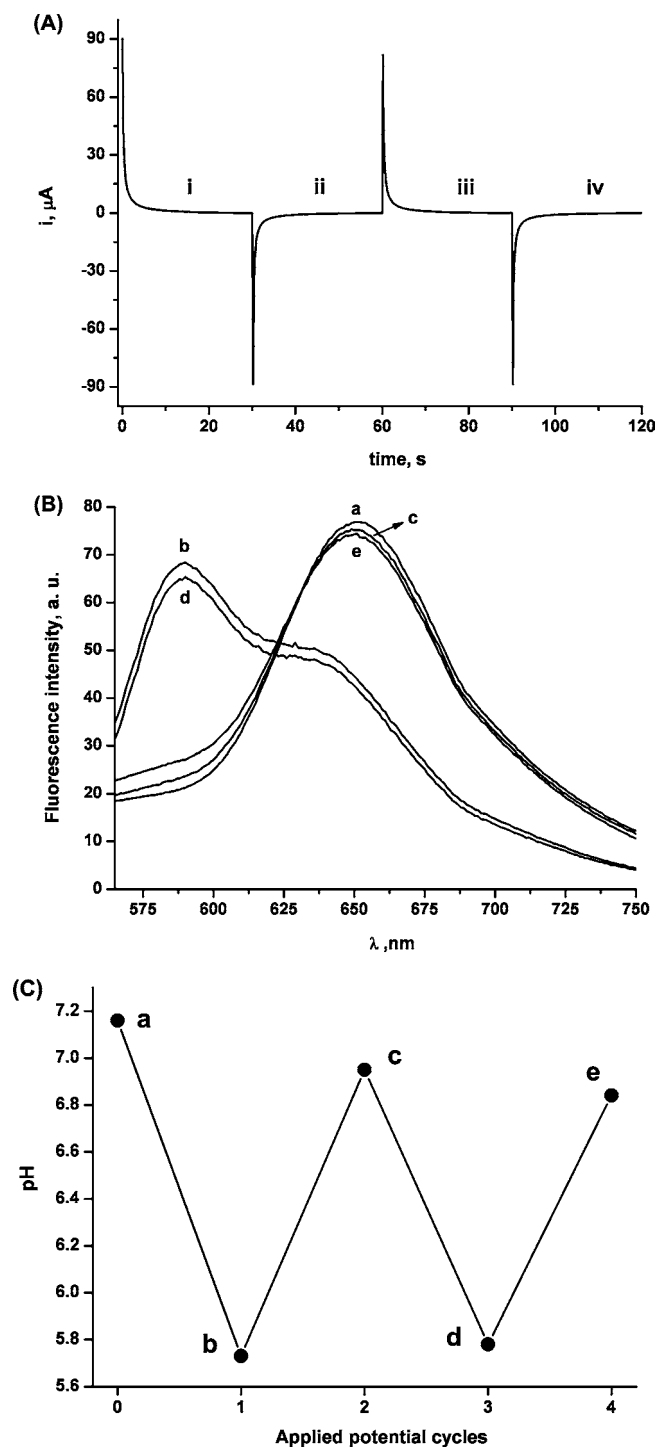


**Figure 4.** (A) Current transient of the bis-aniline-cross-linked Au NPs electropolymerized composite on a Pt black-coated Au electrode upon the application of cyclic oxidation ( $E = 0.25 \text{ V vs SCE}$ , regions (i) and (iii)), and reduction ( $E = -0.05 \text{ V vs SCE}$ , regions (ii) and (iv)) potential pulses in a  $0.5 \text{ M NaCl}$  solution. (B) Emission spectra corresponding to the cyclic electrostimulated pH changes by the bis-aniline-cross-linked Au NPs electropolymerized on a Pt black-coated Au electrode. Curve (a) corresponds to measuring the spectrum of the electrolyte solution, at  $\text{pH} = 7.2$ , before the application of a potential pulse. Curves (b) and (d) correspond to the application of an oxidation potential pulse ( $E = 0.25 \text{ V vs SCE}$  for 30 s). Curves (c) and (e) correspond to the application of a reduction potential pulse ( $E = -0.05 \text{ V vs SCE}$  for 30 s). (C) Cyclic pH changes, upon switching the potential between  $-0.05$  and  $0.25 \text{ V vs SCE}$ , respectively, derived from the fluorescence spectra shown in (B).



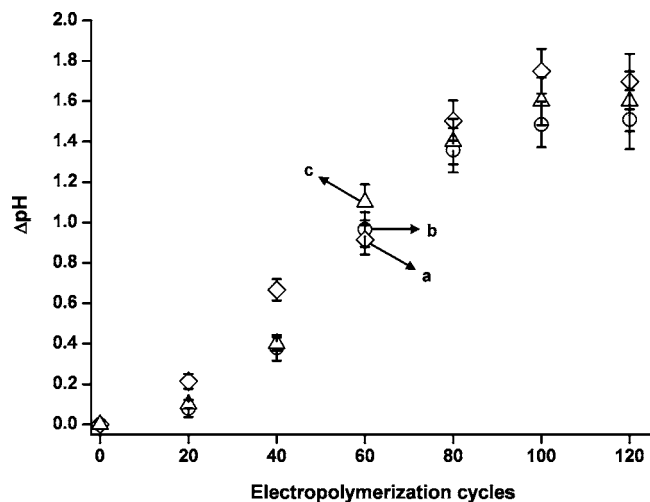


**Figure 5.** Electrostimulated pH changes generated by the bis-aniline-cross-linked Au NPs electropolymerized composite generated by variable numbers of electropolymerization cycles on a Pt black-coated Au electrode. The pH values were derived from the following: (a) marked with (◇), coulometric analysis of the bis-aniline amperometric responses obtained by the application of the oxidation potential pulse; (b) marked with (○), the fluorescence intensities ratio at  $\lambda_1 = 650 \text{ nm}/\lambda_2 = 590 \text{ nm}$  using the carboxy SNARFs dye; (c) marked with (Δ), direct measurement by a pH-meter electrode. Error bars correspond to a set of  $N = 5$  measurements.

electrode. The initial pH of the electrolyte solution was  $\text{pH} = 7.2$ , reflected by the fluorescence band at  $\lambda = 650 \text{ nm}$ , curve (a). Application of the first potential step that oxidizes the bridging units to the quinoid form results in an acidic electrolyte solution,  $\text{pH} = 5.8$ , reflected by the fluorescence band at  $\lambda = 590 \text{ nm}$ , curve (b). The subsequent reduction of the quinoid bridges to the bis-aniline state results in the uptake of protons by the bridging units, and this leads to the regeneration of the pH of the electrolyte (to ca.  $\text{pH} = 7.0$ ), curve (c). Thus, by the cyclic electrochemical oxidation and reduction of the bridges, the pH of the electrolyte solution is reversibly switched between the lower and the higher pH values, Figure 4B, curves (a) to (e) and Figure 4C.

The observed pH changes were, then, correlated with the charge accompanying the redox processes of the bridging units. As stated, the bis-aniline bridging units exhibit a quasi-reversible redox-wave, Figure 1B. As the number of electropolymerization cycles for synthesizing the cross-linked Au NPs increases, the content of the redox-active bridging units in the film is higher. Coulometric analysis of the oxidation wave of the bis-aniline units provides, then, the charge associated upon oxidizing the bridges to the quinoid state and the accompanying release of protons. That is, by the coulometric analysis of the redox wave of the bis-aniline units associated with Au NP composites assembled on the electrode by different numbers of electropolymerization cycles, and assuming that the oxidation of the bis-aniline sites involves the release of two protons, we can calculate the pH changes ( $\Delta\text{pH}$ ), which are anticipated to be generated by the different Au NP composites. Figure 5 shows the calculated  $\Delta\text{pH}$  values generated by the Au NP-functionalized electrodes prepared by the application of variable numbers of electropolymerization cycles, using the coulometric analysis of the bis-aniline oxidation wave, marked with (◇). For comparison, the experimentally electrogenerated pH changes by the respective electrodes using the fluorescence indicator carboxy SNARFs are shown in Figure 5 and marked with (○). The two curves almost overlap, implying that the pH changes, indeed,

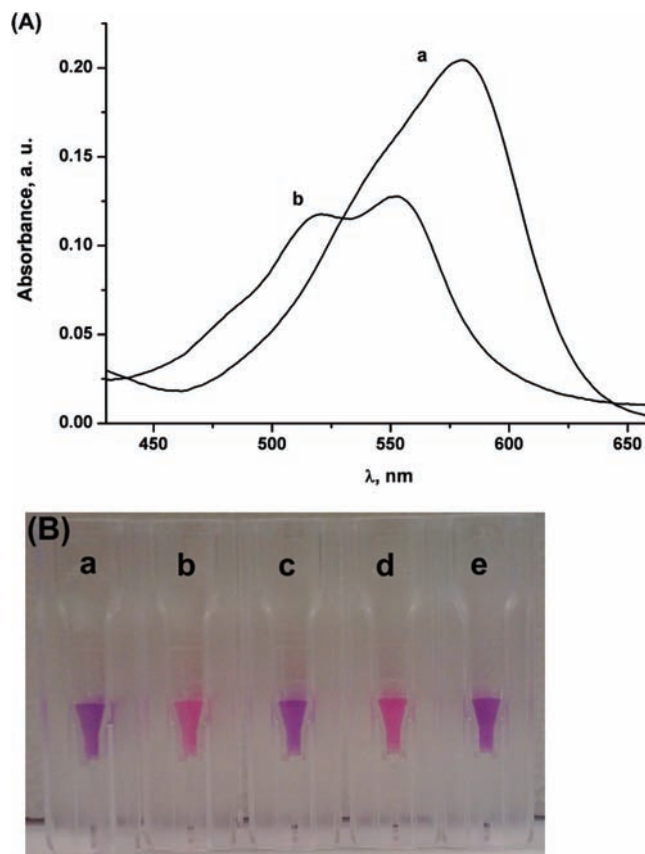


**Figure 6.** (A) UV/visible absorption spectra of the carboxy SNARFs dye,  $5 \mu\text{M}$ , in a  $0.5 \text{ M NaCl}$  solution: (a) before (at  $\text{pH} = 7.2$ ) and (b) after ( $\text{pH} = 5.8$ ) the application of an oxidation potential pulse ( $E = 0.25 \text{ V vs SCE}$  for  $30 \text{ min}$ ) on the bis-aniline-cross-linked Au NPs electropolymerized on a Pt black-coated Au electrode. (B) Solution colors corresponding to the cyclic electrostimulated pH changes generated by the bis-aniline-cross-linked Au NPs electropolymerized on a Pt black-coated Au electrode. Cuvette (a) demonstrates the color of the electrolyte solution (at  $\text{pH} = 7.2$ ) before the application of a potential pulse. Cuvettes (b) and (d) demonstrate the color of the electrolyte solution in (a) and (c), respectively, following the application of an oxidation potential pulse ( $E = 0.25 \text{ V vs SCE}$  for  $30 \text{ s}$ ). Cuvettes (c) and (e) demonstrate the color of the electrolyte solution in (b) and (d), respectively, following the application of a reduction potential pulse ( $E = -0.05 \text{ V vs SCE}$  for  $30 \text{ s}$ ).

originate from the oxidation–reduction process associated with the bis-aniline units. Furthermore, the electrogenerated changes in the pH were, also, directly monitored by a pH-meter, Figure 5, marked with (Δ). We realize that the pH changes analyzed by this method are in excellent agreement with the results obtained by the fluorescent dye and the coulometric analysis of the charge associated with the bridges.

While the fluorescence of the carboxy SNARFs dye provides a sensitive method to follow the pH of the electrolyte solution, the absorbance of this dye is, also, pH-sensitive. Figure 6A shows the absorbance spectra of the dye at  $\text{pH} = 7.2$  and  $\text{pH} = 5.8$ , respectively. This absorption difference allows the visual imaging of the electrostimulated pH changes in the solution upon the oxidation ( $\text{pH} = 5.8$ , pink) and the reduction ( $\text{pH} = 7.2$ , violet) of the bridging units, Figure 6B.

The successful electrochemically stimulated cyclic pH changes allow, in principle, control and switching of the reactivity of chemical or biological processes. To exemplify such processes, we selected the C-quadruplex-stimulated activation of the catalytic functions of a nucleic acid (DNAzyme), as a model

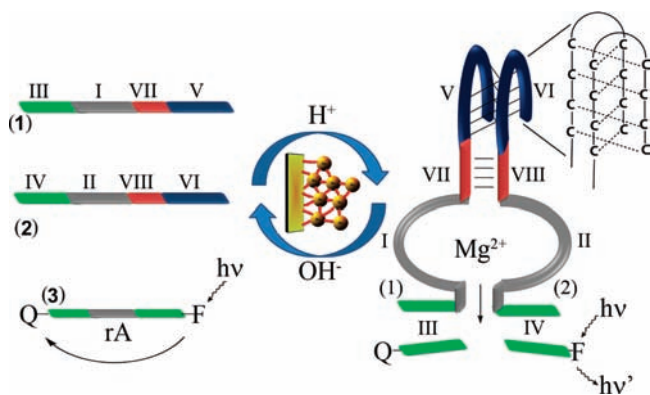


**Figure 7.** The pH-switchable  $\text{Mg}^{2+}$ -DNAzyme subunits, and the reversible ON–OFF electrostimulation of the DNAzyme activity through the formation or dissociation of the C-quadruplex, respectively.

system. Catalytic nucleic acids, DNAzymes,<sup>20</sup> or ribozymes attract growing interest as biocatalytic amplifying units for biosensing events,<sup>21</sup> as active units that control the configuration of nanostructures,<sup>22</sup> and as components that drive logic-gate operations.<sup>23</sup> One of the most studied DNAzyme systems is the E6- $\text{Mg}^{2+}$ -dependent DNAzyme that cleaves a ribonucleobase substrate.<sup>24</sup> Several studies demonstrated that the  $\text{Mg}^{2+}$ -dependent DNAzyme can be cleaved into two subunits and that the subsequent linkage of the two subunits by a coadditive activates its supramolecular structure. For example, the DNAzyme subunits can be reconnected by an added nucleic acid, which enables the activation of the DNAzyme, and this provides a means for the amplified sensing of DNA.<sup>25</sup> Among the different structures of DNA, the C-quadruplex (i-motif) structure is well established.<sup>10,26</sup> At an acidic pH, the C-rich single-stranded DNA self-assembles into the C-quadruplex structure, whereas at a neutral pH, this structure is disrupted. Indeed, pH-stimulated DNA machines (tweezers) were, recently, designed by the formation and disassembly of C-quadruplexes.<sup>27</sup> We have implemented the electrochemically induced pH changes by the bis-aniline Au NPs cross-linked composite to switch-on the  $\text{Mg}^{2+}$ -dependent DNAzyme using the C-quadruplex as activating units for the supramolecular DNAzyme structure, Figure 7. The DNAzyme sequence was cleaved into two subunits, (1) and (2), that include the DNAzyme regions I and II, respectively. The DNAzyme subunits are tethered to the nucleic acid sequences III and IV that are complementary to the substrate (3). The substrate was modified at its 5' and 3' ends with a

fluorophore–quencher pair (ROX and Black Hole 2). It should be noted that the complementarity between domains III and IV in the DNAzyme subunits with the substrate (3) are too weak to stabilize the duplex structures at room temperature (six base pairs). The C-rich nucleic acids V and VI (marked in blue) are tethered to the DNAzyme subunits using the nucleic acid sequences VII and VIII as interlinks. While the subunits (1) and (2) cannot self-assemble into the active  $\text{Mg}^{2+}$ -dependent DNAzyme, the intermolecular C-quadruplex at an acidic pH between the tether units of (1) and (2) could stabilize the  $\text{Mg}^{2+}$ -DNAzyme structure by bringing together the subunits. The electrostimulated oxidation of the bis-aniline units in the Au NP composite-modified electrode is, then, anticipated to acidify the aqueous medium to  $\text{pH} = 5.8$ . At this pH the two DNAzyme subunits self-assemble into the C-quadruplex structure. This links the two subunits together and leads to the synergistic stabilization of the respective duplexes formed between the DNAzyme subunits and the substrate, together with the formation of the active DNAzyme structure. The cleavage of the substrate leads to the release of the fluorophore that provides the readout signal for the biocatalytic process. By the electrostimulated reduction of the bis-aniline bridges, the neutral pH of the system is restored, and this leads to the dissociation of the C-quadruplex and the separation of the DNAzyme subunits into a catalytically inactive structure. It should be noted that the nucleic acid regions VII and VIII in the DNAzyme subunits have an important function in the system. The regions VII and VIII exhibit a six-base complementarity. Although this number of complementary bases is insufficient to form a stable duplex structure at room temperature, this complementarity synergistically stabilizes the C-quadruplex structure between (1) and (2), avoiding the formation of catalytically inactive C-quadruplex structures between (1) and (1) or (2) and (2).

Figure 8 depicts the electrostimulated pH activation of the  $\text{Mg}^{2+}$ -dependent DNAzyme. At  $\text{pH} = 7.2$ , the DNAzyme subunits (1) and (2) and the substrate (3) are present as separated entities, and no active DNAzyme structure is formed. This is reflected by the lack of cleavage of the substrate, which does not generate the fluorescence of the respective fluorophore, Figure 8A, curve (a). The electrochemical change of the pH to 5.8 induces the formation of the C-quadruplex-bridged DNAzyme, and this is reflected by the cleavage of the substrate (3) and the generation of fluorescence, Figure 8A, curve (b). For comparison, the mixture of the DNAzyme subunits (1) and (2) and the substrate (3) was subjected to a pH change from 7.2 to 5.8 by the addition of acid. While at  $\text{pH} = 7.2$  no DNAzyme activity could be detected, at  $\text{pH} = 5.8$ , the components self-assemble into an active DNAzyme structure, that led to the cleavage of (3) and the generation of fluorescence, Figure 8A, curve (c). Control experiments revealed that the activity of the intact  $\text{Mg}^{2+}$ -dependent DNAzyme structure (that includes the complete single-stranded DNAzyme sequence, without the C-quadruplex component) is pH-insensitive in the range of 5.8 to 7.2. Thus, the electrochemically stimulated pH change, indeed, triggers the activation of the  $\text{Mg}^{2+}$ -dependent DNAzyme. Figure 8B shows the switchable electrochemical activation and deactivation of the  $\text{Mg}^{2+}$ -dependent DNAzyme through the electrostimulated pH changes. In this experiment, the DNAzyme subunits (1) and (2) and the substrate (3) act as a reaction mixture in the presence of the modified electrode. Application of the oxidative potential pulse on the electrode results in the release of protons and the acidification of the reaction medium to  $\text{pH} = 5.8$ . This results in the formation of the C-quadruplex-bridged  $\text{Mg}^{2+}$ -dependent

- (20) Silverman, S. K. *Chem. Commun.* **2008**, 3467–3485.  
 (21) (a) Liu, J.; Lu, Y. *J. Am. Chem. Soc.* **2007**, *129*, 9838–9839. (b) Xiao, Y.; Rowe, A. A.; Plaxco, K. W. *J. Am. Chem. Soc.* **2007**, *129*, 262–263. (c) Li, D.; Shlyahovsky, B.; Elbaz, J.; Willner, I. *J. Am. Chem. Soc.* **2007**, *129*, 5804–5805. (d) Elbaz, J.; Shlyahovsky, B.; Willner, I. *Chem. Commun.* **2008**, 1569–1571.  
 (22) Chen, Y.; Wang, M.; Mao, C. *Angew. Chem., Int. Ed.* **2004**, *43*, 3554–3557.  
 (23) (a) Stojanovic, M. N.; Stefanovic, D. *Nat. Biotechnol.* **2003**, *21*, 1069–1074. (b) Moshe, M.; Elbaz, J.; Willner, I. *Nano Lett.* **2009**, *9*, 1196–1200.  
 (24) Breaker, R. R.; Joyce, G. F. *Chem. Biol.* **1995**, *2*, 655–660.  
 (25) (a) Elbaz, J.; Moshe, M.; Shlyahovsky, B.; Willner, I. *Chem.—Eur. J.* **2009**, *15*, 3411–3418. (b) Kolpashchikov, J. D. M. *ChemBioChem* **2007**, *8*, 2039–2042.  
 (26) (a) Liu, H.; Xu, Y.; Li, F.; Yang, Y.; Wang, W.; Song, Y.; Liu, D. *Angew. Chem., Int. Ed.* **2007**, *46*, 2515–2517. (b) Shin, S. R.; Jin, K. S.; Lee, C. K.; Kim, S. I.; Spinks, G. M.; So, I.; Jeon, J.-H.; Kang, T. M.; Mun, J. Y.; Han, S.-S.; Ree, M.; Kim, S. J. *Adv. Mater.* **2009**, *21*, 1907–1910.  
 (27) Elbaz, J.; Wang, Z.-G.; Orbach, R.; Willner, I. *Nano Lett.* **2009**, *9*, 4510–4514.

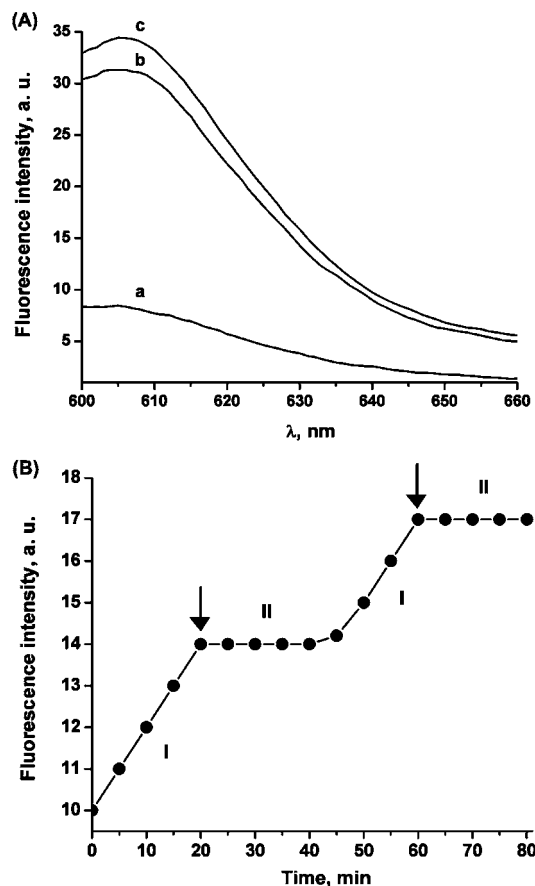


**Figure 8.** (A) Emission spectra corresponding to (a) the  $\text{Mg}^{2+}$ -dependent DNAzyme exposed to a 0.5 M NaCl solution following the application of a reduction pulse ( $E = -0.05$  V vs SCE for 30 s); (b) the  $\text{Mg}^{2+}$ -dependent DNAzyme in (a), following the application of an oxidation pulse ( $E = 0.25$  V vs SCE for 30 s); (c) the  $\text{Mg}^{2+}$ -dependent DNAzyme subunits mixture, exposed to a 0.5 M NaCl solution that was acidified to pH = 5.8 by using HCl. (B) Time-dependent emission corresponding to the  $\text{Mg}^{2+}$ -dependent DNAzyme following the electrochemically induced cyclic decrease (I) and increase (II) in the pH of the solution. In all measurements the excitation wavelength was  $\lambda_{\text{ex}} = 590$  nm. All experiments were performed in a 0.5 M NaCl solution containing 20 mM  $\text{MgCl}_2$  and in the presence of 10  $\mu\text{M}$  of 1, 2, and 3.

DNAzyme that cleaves the substrate (3) and leads to the generation of fluorescence, region I, Figure 8B. At the time indicated, the electrode was subjected to the reductive pulse, resulting in the uptake of protons and the neutralization of the reaction medium to pH = 7.2. This facilitates the separation of the C-quadruplex, the separation of the DNAzyme subunits, and the deactivation of the DNAzyme (region II, Figure 8B). By the repeated electrochemically induced acidification/neutralization of the system, the DNAzyme is cycled between ON and OFF states, respectively.

## Conclusions

The present study has demonstrated the use of a bis-aniline-cross-linked Au NP composite for the cyclic electrochemical control of the pH of an aqueous solution. We demonstrated that the pH can be altered by almost two units. These switched pH changes were the result of two main features of the modified electrode: (i) the electrodeposition of Pt on the bare Au electrode provided a rough surface for the deposition of the bis-aniline-cross-linked Au NP composite; (ii) the content of the bis-aniline-cross-linked Au NP

composite associated with the electrode was controlled by the number of electropolymerization cycles. The modified electrodes were stable for at least one week.

The electrostimulated pH changes were, then, used to control the chemical reactivity of the  $\text{Mg}^{2+}$ -dependent DNAzyme. In principle, many other pH-dependent chemical transformations could be activated by electrical stimuli using such modified electrodes. In fact, one challenging goal would be the electrostimulated pH-driven synthesis of ATP by the motor protein ATPase.

## Experimental Section

**Synthesis of Thioaniline-Modified Au NPs.** Au nanoparticles functionalized with 2-mercaptoethane sulfonic acid and *p*-aminothiophenol were prepared by mixing a 10 mL ethanol solution that included 197 mg of  $\text{HAuCl}_4$  with a 5 mL methanol solution that included 42 mg of mercaptoethane sulfonate and 8 mg of *p*-aminothiophenol. The two solutions were stirred in the presence of 2.5 mL of glacial acetic acid in an ice bath for 1 h. Subsequently, 7.5 mL of an aqueous 1 M sodium borohydride solution were added dropwise to the solution, resulting in a dark color associated with the formation of the Au NPs. The solution was stirred for 1 h in an ice bath and then for 14 h at room temperature. The particles were successively centrifuged and washed with methanol, ethanol, and diethyl ether (twice with each of the solvents). The average size of the NPs was estimated by TEM, to be  $3.6 \pm 0.3$  nm.

**Electropolymerization of the Bis-aniline-Cross-Linked Au NPs Film.** Thioaniline-modified Au NPs ( $2 \text{ mg mL}^{-1}$ ) were dissolved in a HEPES buffer, 10 mM (pH = 7.2). The resulting solution was, then, diluted 6-fold with a phosphate buffer solution, 100 mM (pH = 7.4), and used for the electropolymerization process. Electropolymerization of the thioaniline-modified Au or Pt-coated Au slides was performed by employing a fixed number of cyclic voltammetry scans, in the potential range of  $-0.1$  to  $1.1$  V vs a saturated calomel electrode (SCE), at a scan rate of  $100 \text{ mV s}^{-1}$ .

**Application of the Modified Electrodes To Electrostimulate pH Changes.** The bis-aniline-cross-linked Au NPs-modified Au or Pt black-coated Au electrodes were placed into a 100  $\mu\text{L}$  solution of NaCl, 0.5 M. Prior to the experiments, the pH of this solution was adjusted to pH = 7.2 using NaOH, and the solution was purged with Ar for 30 min. The experiments were conducted in a three-electrode Perspex cell, volume 200  $\mu\text{L}$ . For proton release, a potential pulse of  $E = 0.25$  V vs SCE (or  $E = 0.3$  V vs a Ag wire) was applied for a time interval of 30 s. Similarly, to uptake protons from the aqueous solution, a potential pulse of  $E = -0.05$  V vs SCE (or  $E = 0.0$  V vs a Ag wire) was applied for 30 s. The counter electrode was a graphite rod ( $d = 6$  mm).

Calculation of the pH changes, derived from the coulometric assay of the bis-aniline-cross-linking bridging units, assumed that the oxidation of each bridge resulted in the release of two protons. By applying Faraday's law, the amounts of the generated protons were derived, and these were translated to pH changes, knowing the volume of the cell.

**Chemicals and Instrumentation.** Ultrapure water from a NANOpure Diamond (Barnstead) source was used in all of the experiments. Carboxy seminaphthorhodafluors (carboxy SNARFs) (1) and (2) were purchased from Sigma-Genosys. The oligonucleotide (3) was purchased from Integrated DNA Technologies Inc. (Coralville, IA). The DNA sequences used in the study are

(1) 5' CCC CTT TTC CCC T TA ATG C CA CCC ATG T TA GAG A 3';

(2) 5' C TGC TC A GCG ATG CAT TAT CCC CTT TTC CCC 3';

(3) 5' ROX-TCT CTA TrAG GAG CAG-BH2 3'

All electrochemical experiments were performed using a PC-controlled (Autolab GPES software) electrochemical analyzer potentiostat/galvanostat ( $\mu$ Autolab, type III). Fluorescence measurements were performed using a Cary Eclipse Device (Varian Inc.). A pH-meter electrode (Orion model 320) was used in some of the experiments.

**Acknowledgment.** This research was supported by the EU ECell project.

**Supporting Information Available:** Fluorescence spectra corresponding to the electrostimulated pH changes by the bis-aniline-cross-linked Au NPs electropolymerized for a variable number of electropolymerization cycles on a bare Au electrode are presented. This material is available free of charge via the Internet at <http://pubs.acs.org>.

JA9094796